Phase diagram of the one-dimensional molecular-crystal model with Coulomb interactions: Half-filled-band sector

J. E. Hirsch

Department of Physics, University of California, San Diego, La Jolla, California 92093

(Received 26 April 1984; revised manuscript received 9 October 1984)

We discuss the ground-state phase diagram of the molecular-crystal model for electron-phonon interactions in the presence of on-site (U) and nearest-neighbor (V) electron-electron interactions in the half-filled-band sector. The system is analyzed as a function of the phonon frequency (ω), electron-phonon coupling constant (λ), and U and V in the physically relevant case ($U, V > 0$). We discuss various limiting cases with perturbation theory, as well as intermediate-coupling cases using a numerical simulation technique. In particular, we study in detail the limit $\omega \rightarrow \infty$, which corresponds to the extended Hubbard model. The phase diagram is divided into regions of long-range charge-density-wave (CDW) order, algebraic spin-density-wave (SDW) order, and coexisting algebraic singlet superconducting and CDW order. The transition between CDW and SDW phases is continuous for small U and first order for large U. For the physical parameter range ($U, V > 0$), there is no regime where superconductivity dominates. Modification of this picture for the non-half-filled-band sector is indicated.

I. INTRODUCTION

This is the third of a series of papers in which we discuss the global phase diagram of one-dimensional electron-phonon systems. Such systems have been of great interest in recent years in connection with properties of quasi-one-dimensional organic charge-transfer compounds.[1] A large amount of theoretical effort has been devoted to understanding the competing instabilities in the one-dimensional electron gas, and for the case of nonretarded interactions a coherent picture has emerged. The phase diagram is well understood in the weak-coupling regime from renormalization-group calculations,[2,3] and in the strong-coupling regime[2] from strong-coupling expansions. The intermediate-coupling region is, however, difficult to study theoretically. In addition, the theoretical analysis becomes much more difficult in the presence of retardation (finite phonon frequency) and only recently has progress been made in this direction. In the first two papers of this series[4,5] (hereafter referred to as I and II) we studied the global phase diagram of two one-dimensional electron-phonon systems in the absence of Coulomb interactions: the Su-Schrieffer-Heeger (SSH) model,[6] which considers longitudinal phonons that modify the electronic transfer term, and the molecular-crystal model (Holstein model[7]) in which an intramolecular vibration mode couples to the local electron density. In the present and a forthcoming paper, we consider the models in the presence of electron-electron interactions. In a real quasi-one-dimensional system, usually couplings to various modes of both types of vibrational degrees of freedom will exist.[8] We have not considered both types of couplings simultaneously, although this has been recently done within the mean-field approximation by Kivelson.[9]

In this paper we consider the molecular-crystal model in the presence of an on-site and a nearest-neighbor repulsion U and V,

$$H_{e\text{-ph}} = \sum_i \left[\frac{p_i^2}{2M} + \frac{1}{2} K q_i^2 \right] - t \sum_{i,\sigma} (c_{i\sigma}^\dagger c_{i+1\sigma} + \text{H.c.})$$

$$- \lambda \sum_{i,\sigma} q_i n_{i\sigma} + H_{UV},$$

$$H_{UV} = U \sum_i n_{i\uparrow} n_{i\downarrow} + V \sum_i n_i n_{i+1},$$

(1)

as a function of $\omega = \sqrt{K/M}$, λ, U, and V. $t = 1$ defines the units of energy. We restrict ourselves to the half-filled-band sector. The model equation (1) was studied in paper II in the absence of Coulomb interactions in the half-filled-band sector, and for $U = \infty$ in the quarter-filled-band sector. There it was found that the phase diagram in the half-filled-band case is extremely simple: the model has charge-density-wave (CDW) long-range order for arbitrary λ and $\omega < \infty$, and coexisting algebraic CDW and singlet superconducting (SS) order in the case $\omega = \infty$. In the presence of U and V, the model can also develop algebraic correlations for spin-density-wave (SDW), SS, and TS (triplet superconducting) order. Although in the literature the model in the nonretarded limit is usually discussed for both signs of the interactions U and V, we will here limit ourselves mostly to $U, V > 0$, which is the physical parameter range. A competing *attractive* on-site interaction will arise from the coupling to the phonon degrees of freedom, and no mechanism for an attractive nearest-neighbor interaction exists in the model equation (1). Such an effective attraction would arise from a coupling to nearest-neighbor phonons, but will not be considered here. For the parameter range of interest, the only phases that appear are CDW, SDW, and SS, and nowhere does SS dominate. Thus, our conclusions partly disagree with those of a recent paper by Guinea.[10] In future work we will consider the non-half-filled-band sectors and longer-range electron-phonon couplings, which give the

possibility of dominance of superconducting correlations.

We will first discuss the model in several limiting cases where rigorous theoretical statements can be made: nonretarded regime ($\omega \to \infty$), strong-coupling regime ($\lambda \gg \sqrt{Kt}$), and adiabatic regime ($\omega \to 0$). We then study the model in a nonperturbative way using a Monte Carlo simulation technique.[11] The simulations confirm the theoretical picture obtained from the perturbative analysis and provide quantitative information on the properties of the system in intermediate-coupling regimes. In the limit of large ω, the model reduces to an extended Hubbard model, and we also study this model directly by numerical simulations.

In Sec. II we discuss the properties of the model in the limit of nonretarded interactions ($\omega \to \infty$). In Sec. III we review results on the static limit ($\omega \to 0$) within the mean-field approximation, and in Sec. IV we discuss the strong-coupling regime. In Sec. V we present results of numerical simulations in a low-frequency and a high-frequency regime. In Sec. VI we present results of simulations of the extended Hubbard model, and conclude with some discussion in Sec. VII. Some of the results presented in this paper were reported briefly elsewhere.[12,13]

II. $\omega \to \infty$ REGIME

In the limit of large ω, the phonons can be integrated out, yielding an effective on-site electron-electron attraction $-\lambda^2/K$. This has been discussed in detail in paper II. The Hamiltonian then becomes

$$H = -t \sum_{i,\sigma} (c_{i\sigma}^{\dagger} c_{i+1\sigma} + \text{H.c.}) + U_{\text{eff}} \sum_{i} n_{i\uparrow} n_{i\downarrow}$$
$$+ V \sum_{i} n_i n_{i+1} , \qquad (2)$$

$$U_{\text{eff}} = U - \lambda^2/K . \qquad (3)$$

The properties of this extended Hubbard Hamiltonian have been discussed extensively in the literature. For small U_{eff} and V, we can use the results from the weak-coupling renormalization-group calculations ("g-ology" phase diagram),[2,3] which predict a (continuous) transition between a regime of algebraic SDW order for $U_{\text{eff}} > 2V$, to long-range CDW order for $U_{\text{eff}} < 2V$. For negative U_{eff} the system can have algebraic singlet or triplet superconducting pairing only for $V \leq 0$. The g-ology phase diagram in the half-filled-band case is shown in Fig. 1, in terms of the real-space parameters U_{eff} and V. In the physical parameter range ($U, V > 0$) the system can only have CDW long-range order, SDW algebraic order, or CDW and SS coexisting algebraic order (for $U_{\text{eff}} < 0$, $V = 0$).

The features shown in Fig. 1 actually persist in strong coupling also. For large and negative U_{eff}, a strong-coupling expansion yields coexisting SS and CDW instabilities for $V = 0$ and dominance of one or the other for $V < 0$ and $V > 0$, respectively.[2] For large and positive U_{eff} and V it is clear that the ground state consists of either pairs occupying alternating lattice sites or all singly occupied sites, as shown in Fig. 2. From considering the
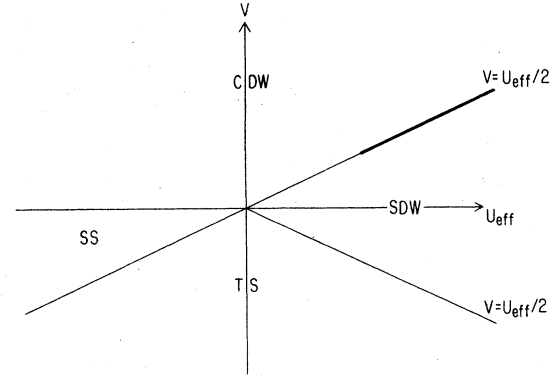

FIG. 1. Schematic phase diagram of the extended Hubbard model in the half-filled-band sector. The bold line denotes a discontinuous transition.

energy of those configurations, one finds the transition to occur at $V = U_{\text{eff}}/2$. For $V > U_{\text{eff}}/2$ the ground state is doubly degenerate with a CDW of period 2. For $V < U_{\text{eff}}/2$ the system is described by a Heisenberg model with coupling $J_{\text{eff}} = t^2/(U_{\text{eff}} - V)$, so that the ground state has algebraic SDW order. However, the transition line $V = U/2$ in Fig. 1 is only asymptotically correct in weak and strong coupling. For intermediate couplings we find that it deviates towards larger V, so that the SDW region is slightly enlarged, as will be shown in Sec. VI.

It is interesting to discuss the order of the transition from the CDW to the SDW state. In the weak-coupling regime, the transition predicted by g-ology is continuous (infinite order). However, in the limit $t \ll U_{\text{eff}}, V$, it is clear that the transition is discontinuous (first order). Consider the system close to the transition for $V > U_{\text{eff}}/2$, i.e., in the CDW state. The low-lying excitations are "droplets" of the SDW phase with energy

$$\epsilon(n) = V - n(U_{\text{eff}} - 2V) \qquad (4)$$

for a droplet of size n. V is the surface energy, which is the dominant term for small n. If we now let V become smaller than the critical value, there will be a critical droplet size

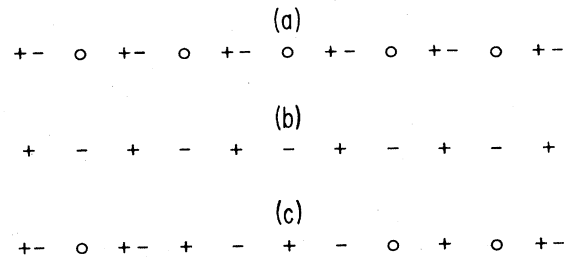$$n_{\text{crit}} = \frac{V}{U_{\text{eff}} - 2V} , \qquad (5)$$

FIG. 2. Extended Hubbard model in the strong-coupling regime. (a) CDW ground state, for $V > U_{\text{eff}}/2$. (b) SDW ground state (schematic), for $V < U_{\text{eff}}/2$. (c) Droplet of SDW phase in CDW background.

such that droplets with $n > n_{crit}$ are energetically favored and the system will tunnel to the other phase by nucleation. This will happen if the hopping amplitude t, which plays the role of temperature, is nonzero. This clearly describes a first-order transition. For a finite value of the hopping t, the droplet energy is lowered by the kinetic-energy term, since a droplet of size n can occupy $n + 1$ sites, as shown in Fig. 2. The kinetic-energy lowering is proportional to t, and is presumably only weakly dependent on the size of the droplet, so that we can think of it as a surface term. It plays a role analogous to the entropy of the droplet boundary in a classical model. The energy of a droplet is then

$$\epsilon(n) = V - ct - n(U_{eff} - 2V), \tag{6}$$

with c a constant. For $V \sim t$ the two surface contributions cancel and it becomes advantageous to nucleate many droplets of arbitrary size, as V is reduced below $U_{eff}/2$, so that the transition becomes continuous.[14]

For $\omega < \infty$ the effective interaction between the electrons becomes retarded. From the arguments given in paper II, we believe that the system for $U_{eff} < 0$, $V = 0$ will move from the coexistence line towards the CDW region in Fig. 1 for any $\omega < \infty$. Recently, Caron and Borbounnais[15] showed this to be the case for $\omega < t$ within a two-cutoff renormalization-group scheme.[16] However, that scheme predicts that the system remains on the coexistence line if $\omega > t$, which is in disagreement with Monte Carlo simulations as well as with results from the strong-coupling expansion.

III. $\omega \rightarrow 0$ LIMIT

In the $\omega \rightarrow 0$ limit one considers the static phonon configuration that minimizes the total ground-state energy. For $U, V = 0$ the problem can, of course, be solved exactly, and one finds a CDW state for any $\lambda > 0$. For $U, V \neq 0$ no exact solution exists, but the problem has been studied within the mean-field approximation.[17] Mean-field theory gives a discontinuous transition at

$$U - \lambda^2/K = 2V \tag{7}$$

between a CDW and a SDW state. Note that this agrees with the results in the large-ω limit for $V > 0$, except that here the transition is predicted to be always discontinuous. However, this is probably an artifact of the mean-field approximation. The main difference with the regime $\omega \rightarrow \infty$ is that here the case $U - \lambda^2/K) < 0$, $V = 0$ has long-range CDW order instead of coexisting CDW and SS order. As mentioned before, we believe the same qualitative behavior obtained for $\omega = 0$ should hold for any $\omega < \infty$.

IV. STRONG-COUPLING REGIME

We consider here an expansion in the hopping matrix element t for arbitrary phonon frequency ω. The Hamiltonian for one site is

$$H_j = \frac{p_j^2}{2M} + \frac{1}{2}K[q_j + (\lambda/K)(n_{j\uparrow} + n_{j\downarrow})]^2$$
$$- (\lambda^2/K - U)n_{j\uparrow}n_{j\downarrow}, \tag{8}$$

up to chemical potential terms. The presence of the electrons shifts the equilibrium position of the oscillator to $-q_0/2$ or $-q_0$, with

$$q_0 = \lambda/K, \tag{9}$$

depending on whether the site is singly or doubly occupied. The starting point of the expansion depends on the relative magnitude of the parameters. As discussed in Sec. II, the ground state for $t = 0$ is a CDW state for

(a) $\quad V > \frac{1}{2}(U - \lambda^2/K), \tag{10}$

and it has only singly occupied sites if

(b) $\quad V < \frac{1}{2}(U - \lambda^2/K). \tag{11}$

In case (a) the ground state is highly degenerate if $V = 0$, since the $N/2$ pairs can be distributed arbitrarily over N sites. In that case, the expansion discussed in paper II is applicable and one obtains

$$H_{eff} = -\tilde{t}\sum_i(\tilde{b}_i^\dagger\tilde{b}_{i+1} + \text{H.c.}) + \tilde{V}\sum_i\tilde{n}_i\tilde{n}_{i+1}, \tag{12}$$

where $\tilde{b}_i^\dagger$ is a small-polaron operator that creates a pair of electrons and shifts the equilibrium position of the oscillator from 0 to $-q_0$. The parameters are given by

$$\tilde{t} = \frac{2t^2}{\omega}e^{-4g}\sum_{n,n'}(-1)^{n+n'}\frac{(2g)^{n+n'}}{n!n'!}\frac{1}{n+n'+4g}, \tag{13}$$

$$\tilde{V} = \frac{4t^2}{4\omega}e^{-4g}\sum_{n,n'}\frac{(2g)^{n+n'}}{n!n'!}\frac{1}{n+n'+4g}, \tag{14}$$

with

$$g = \frac{1}{4\omega}\left[\frac{\lambda^2}{K} - U\right]. \tag{15}$$

For any $\omega < \infty$, one has $\tilde{V} > 2\tilde{t}$, so that the ground state is a CDW state, as discussed in paper II for $U = 0$. In the presence of a small $V > 0$, its effect to lowest order is to shift $\tilde{V} \rightarrow \tilde{V} + 4V$, so that the CDW state is even more enhanced. We conclude then that, for $\lambda^2/K - U \gg t$, the ground state is a CDW state for arbitrary values of ω and $V \geq 0$.

For case (b) the strong-coupling expansion parallels the calculation by Beni, Pincus, and Kanamori.[18] The ground state has only singly occupied sites, and in second order one generates an isotropic spin-spin interaction,

$$H_{eff} = 2J_{eff}\sum_i \mathbf{S}_i \cdot \mathbf{S}_{i+1}, \tag{16}$$

with $\mathbf{S}_i$ the usual spin-$\frac{1}{2}$ operators, and J_{eff} of the same form as $\tilde{t}$ in Eq. (11), but with

$$g = \frac{1}{4\omega}\left[U - \frac{\lambda^2}{K} - V\right]. \tag{17}$$

Thus, the effect of V is only to enhance the exchange coupling J_{eff}, but it does not change the behavior of the spin correlation functions. In the limit $\omega \rightarrow \infty$, Eqs. (13) and (17) yield

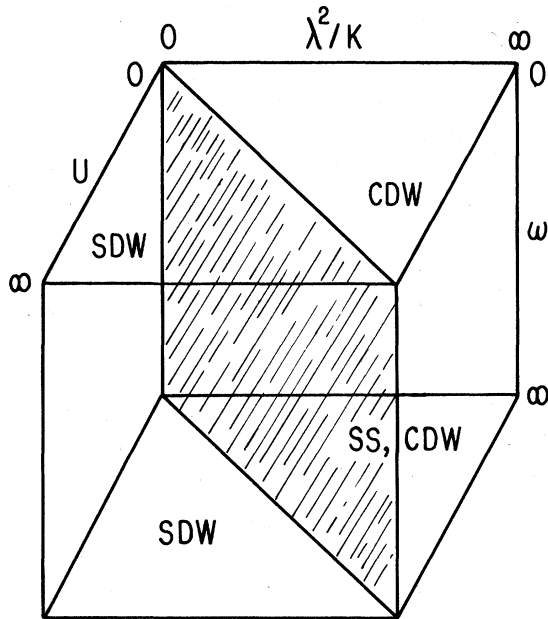$$J_{eff} = \frac{t^2}{U - \lambda^2/K - V}, \tag{18}$$

FIG. 3. Schematic phase diagram of the molecular crystal model. For $\omega < \infty$ the ground state is either CDW or SDW. For $\omega = \infty$ the ground state is SDW or coexisting SS and CDW.

FIG. 5. Zero-frequency SDW susceptibility for various values of U, $\omega = 0.1$.

as one would expect. As ω decreases, J_{eff} becomes smaller, as is seen from Eq. (13). The size of J_{eff} determines for which temperatures one is approaching the low-temperature regime of the Hamiltonian (16). In summary, we find that within strong coupling we obtain a CDW state for case (a) [Eq. (10)] and a SDW state for case (b) [Eq. (11)] for arbitrary $\omega < \infty$. Since this is the same result obtained from the mean-field approximation in the $\omega = 0$ limit, we conclude that for any $\omega < \infty$ the behavior of the system is qualitatively similar.

In Fig. 3 we show the schematic phase diagram that emerges from the preceding considerations. The vertical plane separating the two phases obeys the equation $U - \lambda^2/K = 0$ for all ω. The only qualitative effect of ω is to yield coexisting SS and CDW algebraic phases at $\omega = \infty$ if $V = 0$. For $V > 0$, the phase diagram is the same if we replace λ^2/K by $\lambda^2/K + 2V$, except that even for $\omega = \infty$ there is long-range CDW order in that case.

V. NUMERICAL SIMULATIONS FOR FINITE ω

In this section we discuss results of numerical simulations of the molecular-crystal model in the presence of U

and V. The technique has been discussed in detail elsewhere,[11] and numerical results for the case $U = V = 0$ were presented in paper II. Here we are mainly interested in the effect of U and V on the CDW and SDW correlations. Most simulations were carried out on lattices of spatial size 24 with "time slice" $\Delta\tau = 0.25$, and electron-phonon coupling constant $\lambda = 0.636$. Our purpose is to verify that the simple picture that emerges from the theoretical considerations in limiting cases also holds qualitatively for intermediate parameter regimes, and also to check its quantitative accuracy.

Typical simulations involved 10 000—25 000 sweeps through the lattice, attempting to update the phonon field three times at each point. We usually started the lattice in a dimerized configuration. Because the system takes a very long time to equilibrate, we repeated the simulations several times with different initial dimerization, until it appeared that there was no significant drift in the results.[19]

We first consider a case of small ionic frequency, $\omega = \sqrt{K/M} = 0.1$. Figure 4 shows the decay of the lattice staggered correlation function,

FIG. 4. Decay of scattered correlation functions vs distance for various values of U and $\omega = 0.1$. Here and in the following figures, $\lambda = 0.636$, $K = 0.25$, and $t = 1$. (a) Lattice-displacement correlation function. (b) Electron-density correlation function.
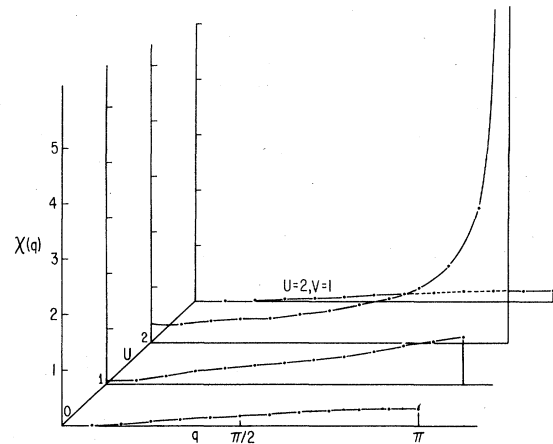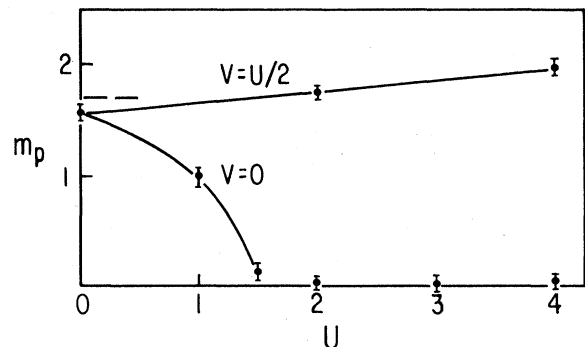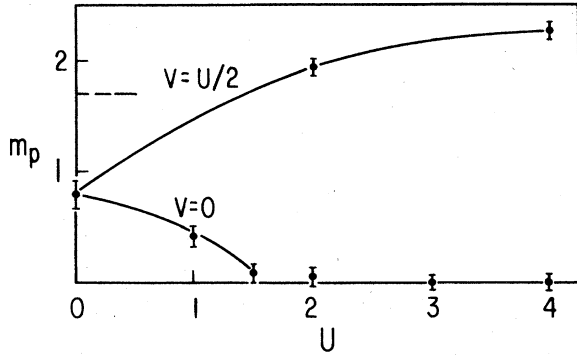

FIG. 6. Lattice dimerization vs U, $\omega = 0.1$. The dashed line is the $\omega = 0$ result for $U, V = 0$.

FIG. 7. Lattice dimerization vs U, $\omega=1$.

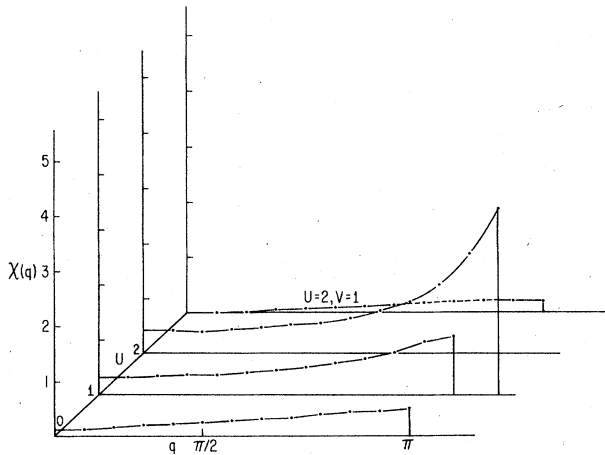$$D_p(l)=\frac{1}{N}\sum_j(-1)^l\langle q_jq_{j+l}\rangle \, , \qquad (19)$$

and the electron-density staggered correlation function,

$$D_e(l)=\frac{1}{N}\sum_{j,\sigma,\sigma'}(-1)^l(\langle n_{j\sigma}n_{j+l\sigma'}\rangle-\langle n_{j\sigma}\rangle\langle n_{j+l\sigma'}\rangle) \, , \qquad (20)$$

versus l for the case $\lambda=0.636$, $K=0.25$, $t=1$, and $V=0$. The temperature was taken to be $T=0.055<\omega$, so that fluctuations are predominantly quantum rather than thermal. Note the somewhat reduced long-range order from the limit $\omega=0$ due to quantum fluctuations for $U=0$. The long-range order clearly persists for $U=1$ and vanishes for $U=2$.

Figure 5 shows the zero-frequency Fourier-transformed SDW susceptibility, defined by

$$\chi(q)=\frac{1}{N}\int d\tau\sum_{j,l}\langle\,[n_{j\uparrow}(\tau)-n_{j\downarrow}(\tau)]$$

$$\times[n_{j+l,\uparrow}(0)-n_{j+l,\downarrow}(0)]\rangle e^{iql} \, . \qquad (21)$$

FIG. 8. Zero-frequency SDW susceptibility, $\omega=1$.
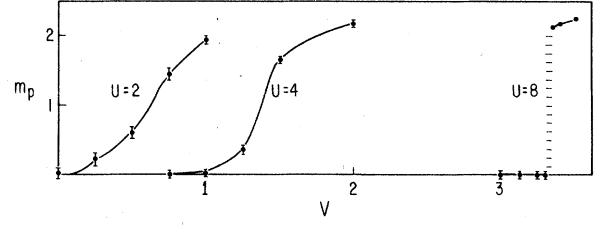
FIG. 9. Lattice dimerization vs V for various U, $\omega=1$. Note how the transition becomes sharper as U increases, and is discontinuous for $U=8$.

The spin susceptibility is very small for the cases where there is CDW long-range order, and increases dramatically when the long-range order disappears. Figures 4 and 5 strongly suggest that there is no coexistence of CDW and SDW regimes.

Figure 6 shows the lattice dimerization,

$$m_p=\frac{1}{N}\sum_j(-1)^j\langle q_j\rangle \, , \qquad (22)$$

versus U for the cases $V=0$ and $V=U/2$. For $V=0$ the point where the dimerization vanishes agrees with the prediction of mean-field theory, $U_c=\lambda^2/K=1.62$, within errors. For $V=U/2$ the numerical results show that the dimerization increases slowly with U, while mean-field theory would predict no change in that case.

Figure 7 shows the behavior of the dimerization versus U for a case of large ionic frequency, $\omega=1$. The temperature in this case was $T=0.167$. The order is greatly reduced due to quantum fluctuations. It appears, however, that the effect of U in suppressing the long-range order is similar to the case of small ω, and within our numerical errors the large-ω prediction that CDW disappears at $U=\lambda^2/K$ appears to hold. Again, for finite V the order is enhanced, and in this case even more than for the small-ω case. Figure 8 shows the spin susceptibility for this case. Again, it grows as the CDW order disappears, but it is substantially smaller here in the case $U=2$ than for the small-ω case. We can understand this from the theoretical considerations: For $\omega\to\infty$ the phonons yield an effective attractive interaction that is subtracted from U, so that $U_{\text{eff}}=0.4$ only for this case. In contrast, in the
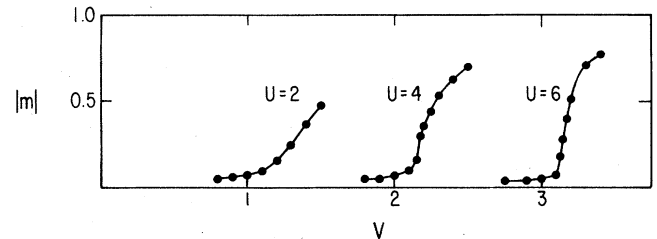
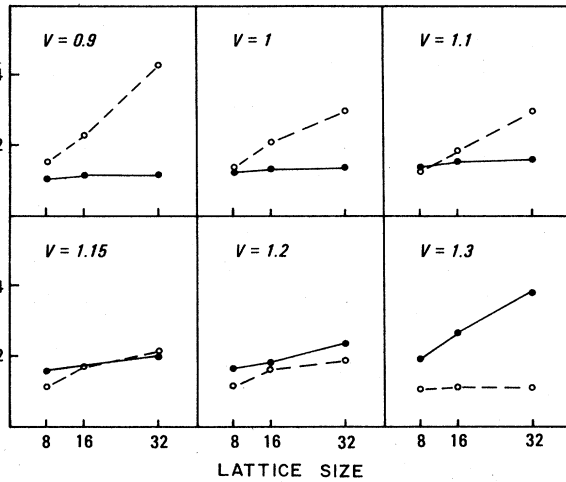FIG. 10. Absolute value of CDW order parameter vs V for $U=2$, 4, and 6 for a 32×32 lattice, $\beta=8$.
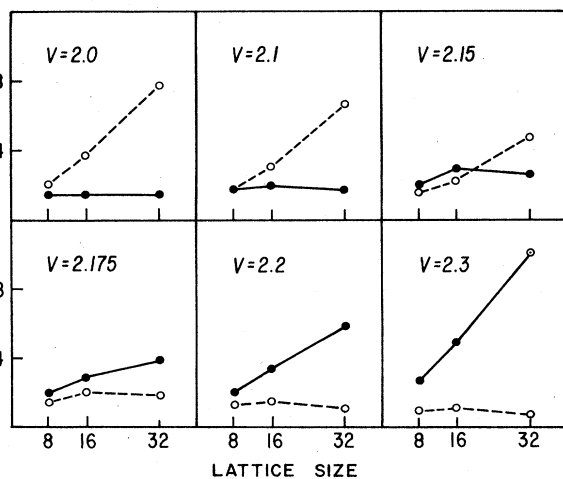
FIG. 11. CDW structure factor (solid line) and SDW suscep-
tibility (dashed line) vs lattice size for $U = 2$ and several values
of V.

$\omega \rightarrow 0$ limit, when the long-range CDW disappears, the
phonons have essentially no effect and the SDW response
is essentially given by its value in the Hubbard model for
$U = 2$.

In Fig. 9 we show results for the dimerization versus V
for $U = 2$, 4, and 8 in the case $\omega = 1$. Note how the transi-
tion becomes sharper as U increases, and is clearly discon-
tinuous for $U = 8$. The transition there occurs at
$V_c \sim 3.32 \pm 0.05$, slightly larger than the expected mean-
field value $V = \frac{1}{2}(U - \lambda^2/K) = 3.19$. The results for
$U = 8$ were obtained by starting the simulations in a
"mixed phase,"[20] with one-half of the lattice in the CDW
phase and one-half in the SDW phase. If the simulations
were started in one of the ordered phases, the system

FIG. 12. CDW structure factor (solid line) and SDW suscep-
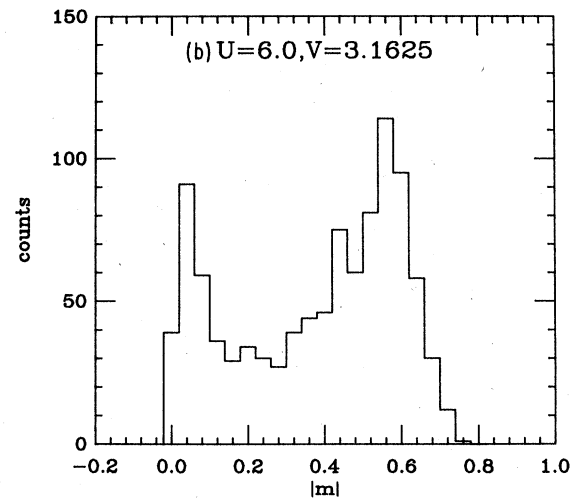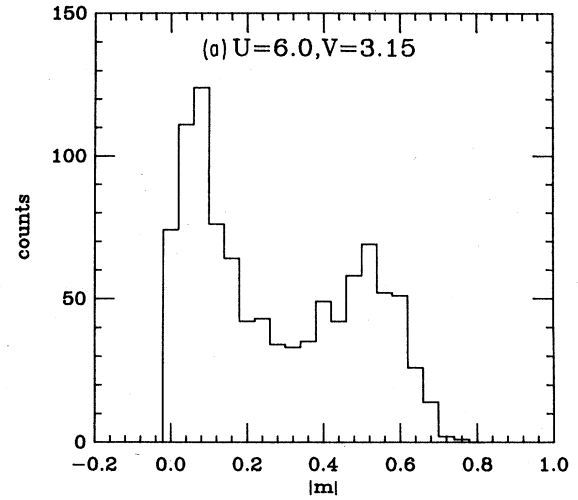tibility (dashed line) vs lattice size for $U = 4$ and several values
of V.

FIG. 13. Histograms of the absolute value of the CDW order
parameter for $U = 6$ and two values of V on a 32×32 lattice.

remained in it even away from the transition point due to
metastability. However, comparison of the energies for
the system in both phases allowed an accurate determina-
tion of the transition point. Figure 9 shows that the tran-
sition goes from continuous to discontinuous as U is in-
creased, in accordance with the discussion in Sec. II.

VI. NUMERICAL SIMULATIONS
FOR THE EXTENDED HUBBARD MODEL

In this section we discuss results of simulations of the
extended Hubbard model, which corresponds to the
large-ω limit of the molecular-crystal model. Figure 10
shows results for the average CDW order parameter

$$m = \frac{1}{N}\sum_i (-1)^i n_i \tag{23}$$

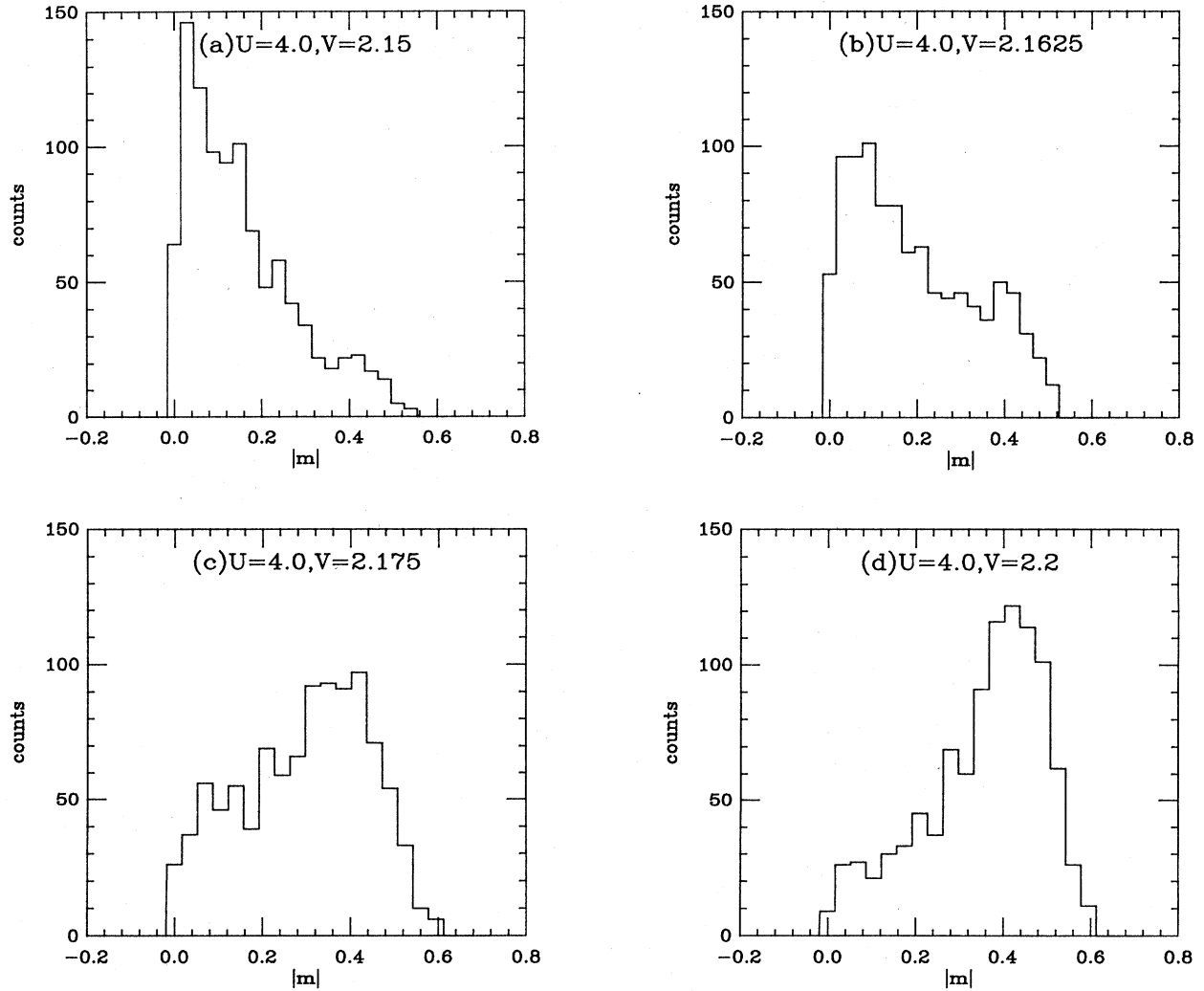for various values of U. Just as in the case of finite ω, the

FIG. 14. Histograms of the absolute value of the CDW order parameter for $U=4$ and several values of V on a 32×32 lattice.

transition becomes sharper as U is increased; it can also be seen that the transition occurs at a slightly larger value of V than the theoretical prediction $V=U/2$.

In order to determine the transition point accurately, we studied the equal-time CDW structure factor

$$S(q)=\frac{1}{N}\sum_{i,j}e^{iq(R_i-R_j)}\langle n_i n_j\rangle \ , \qquad (24)$$

and the zero-frequency SDW susceptibility

$$\chi(q)=\frac{1}{N}\int_0^\beta d\tau\sum_{i,j}\langle[n_{i\uparrow}(\tau)-n_{i\downarrow}(\tau)][n_{j\uparrow}(0)-n_{j\downarrow}(0)]\rangle \ , \qquad (25)$$

for different lattice sizes and temperatures. If we scale the spatial size N and the inverse temperature β by the same factor, $S(q=\pi)$ will diverge linearly with N if we are in the CDW phase, and $\chi(q=\pi)$ will diverge linearly in the SDW phase. Figures 11 and 12 show results for

$U=2$ and $U=4$. These indicate clearly that the transition point is shifted from $V=U/2$ to larger values of V. From these and other simulations we estimate the transition points to be $V=1.15$ for $U=2$, $V=1.675$ for $U=3$, $V=2.163$ for $U=4$, $V=3.158$ for $U=6$, and $V=4.131$ for $U=8$.

To determine the character of the transition, we have studied hysteresis cycles and histograms of the order parameter. In cycles where we first increase and then decrease the value of V, we clearly see increasing hysteresis as U is increased,[13] indicating that the transition is turning first order. They do not, however, provide a precise quantitative criterion on the character of the transition since the presence or absence of hysteresis is strongly dependent on the speed with which we sweep through the transition.

Figure 13 shows histograms of the absolute value of the CDW order parameter for $U=6$. The two coexisting peaks clearly indicate that the transition is strongly first order here. Figure 14 shows histograms for $U=4$ and
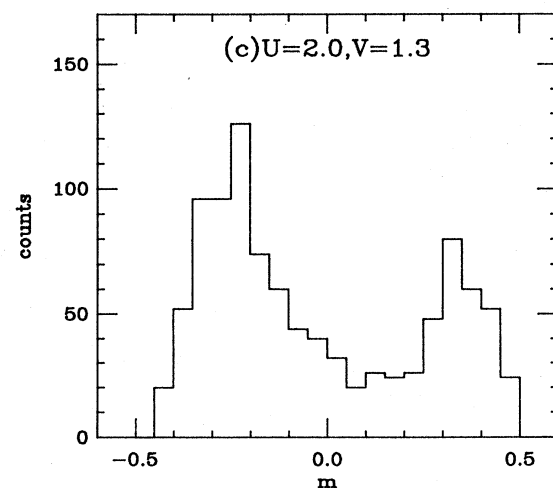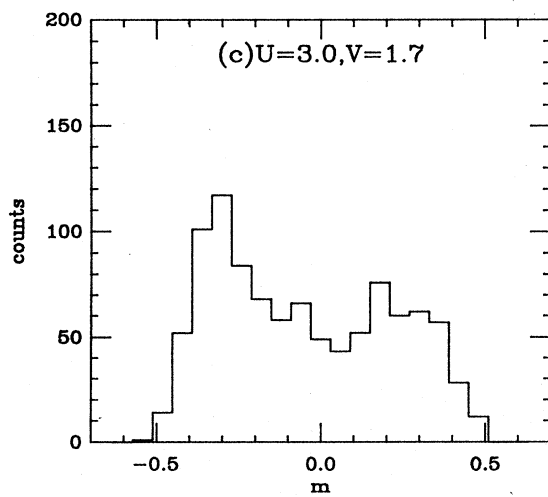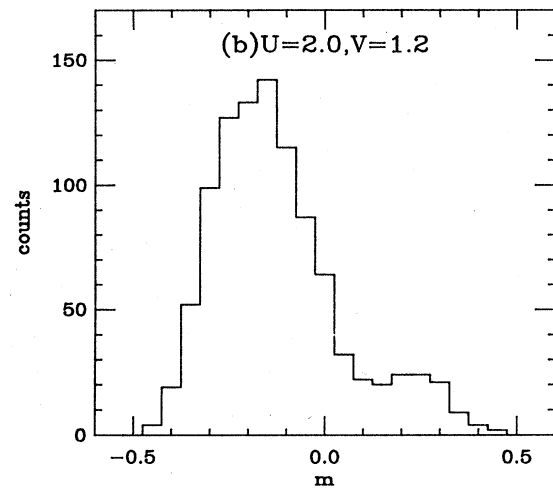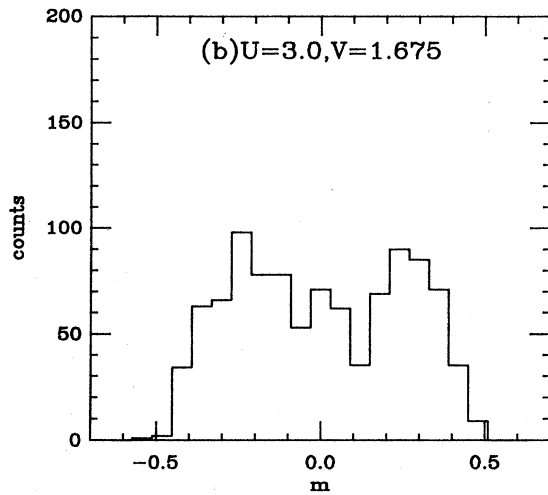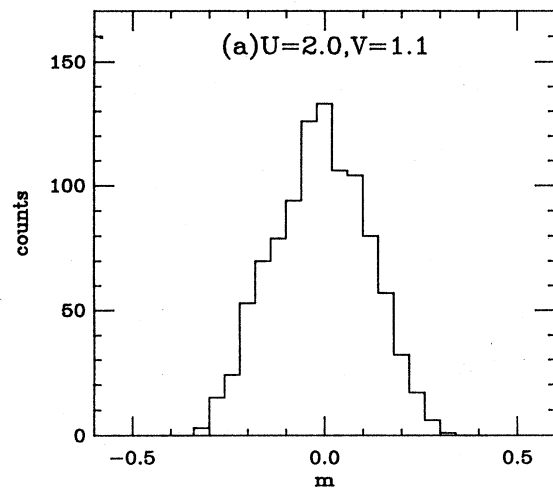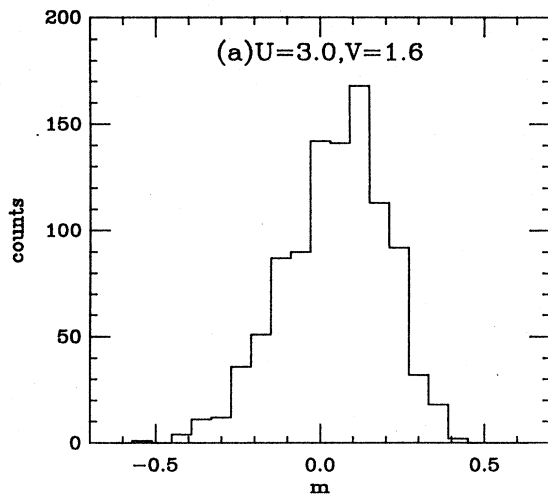
FIG. 15. Histograms of the CDW order parameter for $U = 3$ and several values of V on a 32×32 lattice.

FIG. 16. Histograms of the CDW order parameter for $U = 2$ and several values of V on a 32×32 lattice.
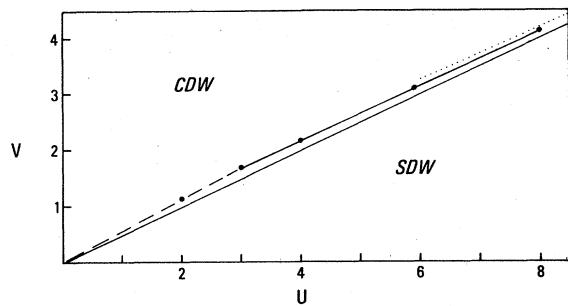
FIG. 17. Phase boundary between CDW and SDW regions. The solid line denotes $U=2V$; the dotted line denotes predictions of strong-coupling perturbation theory. The dashed and solid lines connecting the Monte Carlo points indicate continuous and first-order transitions, respectively.

$V=2.1$, 2.1625, 2.175, and 2.2. Note that the transition is still extremely sharp, and we still see some coexistence of the two phases. In Fig. 15 we show results for $U=3$. The peaks here are broader, but there is still some indication of coexistence of the two phases for $V=1.675$. Finally, for $U=2$ (Fig. 16) we see a broad peak that shifts continuously as V is increased. We conclude from these and other simulations that the transition becomes discontinuous around $U=3$, or slightly below, and becomes rapidly strongly first order as U is increased.

The transition line obtained from our simulations is shown in Fig. 17. For finite ω we expect a similar shift from the $U_{\text{eff}}=2V$ line towards the CDW phase, as was found in Fig. 9. It is easy to understand this shift due to the larger entropy of the SDW phase: For $t=0$ there are only two degenerate CDW ground states, but $\binom{N}{N/2}$ degenerate SDW states. From strong-coupling perturbation theory, we obtained the phase boundary shown as the dotted line in Fig. 16.[13]

VII. CONCLUSIONS

From the analytical and numerical results discussed in this paper, we believe we have established the main features of the phase diagram of the molecular-crystal model in the half-filled-band case for all values of the coupling constants. Our main results for the case of repulsive on-site and nearest-neighbor interactions are summarized as follows:

(a) There is no regime where superconducting correla-

tions dominate. In fact, SS correlations only decay algebraically if $\omega=\infty$, with the same power as CDW correlations if $U<\lambda^2/K$ and $V=0$.

(b) There is a transition between CDW and SDW regions at $U \sim U_c = 2V+\lambda^2/K$. The transition actually occurs at $U=U_c$ for weak and strong coupling, but deviates slightly towards smaller U for intermediate couplings.

(c) The phonon frequency plays a relatively minor role, unlike the case of the SSH model. It does not modify the qualitative features of the phase diagram, except in the limiting case $\omega=\infty$. Its main effect is to reduce the size of both SDW and CDW correlations with respect to the $\omega=0$ limit.

(d) The transition between CDW and SDW phases can be continuous or discontinuous; in particular, it becomes discontinuous for large values of U. For the extended Hubbard model, the crossover occurs around $U \sim 3$.

It is clear that the parameter regime discussed in these pages is particularly unfavorable for superconducting correlations. It is easy to see that a non-half-filled-band case would allow the possibility of dominant SS correlations in certain regions of parameter space. We have recently studied this question in a related model involving excitonic instead of vibronic degrees of freedom.[21] In addition, one can show that coupling to nearest-neighbor phonon degrees of freedom would enhance SS correlations.

In summary, from the analytical and numerical results discussed here, we have obtained a coherent picture of the global phase diagram of the molecular-crystal model in the presence of short-range electron-electron interactions. We have also obtained new information on the phase diagram of the extended Hubbard model. We believe our results should be useful to interpret properties of various quasi-one-dimensional materials that can be described approximately by the model discussed here.

[1]See, for example, *Recent Developments in Condensed Matter Physics*, edited by J. Devreese (Plenum, New York, 1981), Vol. 1, Chap. 8, and references therein.

[2]V. J. Emery, in *Highly Conducting One-Dimensional Solids*, edited by J. Devreese, R. Evrard, and V. van Doren (Plenum, New York, 1979).

[3]J. Solyom, Adv. Phys. 21, 201 (1979).

[4]E. Fradkin and J. E. Hirsch, Phys. Rev. B 27, 1680 (1983).

[5]J. E. Hirsch and E. Fradkin, Phys. Rev. B 27, 4302 (1983).

[6]W. P. Su, J. R. Schrieffer, and A. J. Heeger, Phys. Rev. B 22, 2099 (1980).

[7]T. Holstein, Ann. Phys. (N.Y.) 8, 325 (1959).

[8]E. Conwell, Phys. Rev. B 22, 1761 (1980).

[9]S. Kivelson, Phys. Rev. B 28, 2653 (1983).

[10]F. Guinea, J. Phys. C 16, 4405 (1983).

[11]J. E. Hirsch, D. J. Scalapino, R. L. Sugar, and R. Blanckenbecler, Phys. Rev. B 26, 5033 (1982).

[12]J. E. Hirsch, Phys. Rev. Lett. 51, 296 (1983).

[13]J. E. Hirsch, Phys. Rev. Lett. 53, 2327 (1984).

[14]D. Haldane first predicted the crossover from continuous to first-order transition in the extended Hubbard model using weak-coupling arguments (private communication).

[15]L. G. Caron and C. Borbounnais, Phys. Rev. B 29, 4230 (1984).

[16]G. S. Grest, E. Abrahams, S. T. Chui, P. A. Lee, and Z. Zawadowski, Phys. Rev. B 14, 1225 (1976).

[17]S. K. Chan and V. Heine, J. Phys. F 3, 795 (1973).

[18]G. Beni, P. Pincus, and J. Kanamori, Phys. Rev. B 10, 1896 (1974).

[19]One of the data reported in Ref. 12, for $U=2$, was actually significantly in error, since the system had not reached equilibrium. We now find, upon repeating that run several times, that there is no long-range dimerization order for that case (Figs. 4 and 6).

[20]M. Creutz, L. Jacobs, and C. Rebbi, Phys. Rev. D 20, 1915 (1979).

[21]J. E. Hirsch and D. J. Scalapino, Phys. Rev. Lett. 53, 706 (1984).